Article

The Knudsen Paradox in Micro-Channel Poiseuille Flows with a Symmetric Particle

Ananda Subramani Kannan [1,*], **Tejas Sharma Bangalore Narahari** [1], **Yashas Bharadhwaj** [1], **Andreas Mark** [2], **Gaetano Sardina** [1], **Dario Maggiolo** [1], **Srdjan Sasic** [1] and **Henrik Ström** [1]

[1] Department of Mechanics and Maritime Sciences, Division of Fluid Dynamics, Chalmers University of Technology, 412 96 Göteborg, Sweden; tejass@student.chalmers.se (T.S.B.N.); yashas@student.chalmers.se (Y.B.); sardina@chalmers.se (G.S.); maggiolo@chalmers.se (D.M.); srdjan@chalmers.se (S.S.); henrik.strom@chalmers.se (H.S.)

[2] Fraunhofer-Chalmers Research Centre, 412 88 Göteborg, Sweden; andreas.mark@fcc.chalmers.se

[*] Correspondence: ananda@chalmers.se

Featured Application: The present work addresses a perceived knowledge gap in rarefied flows, along with a relevant challenge while modeling gas–solid flows in confined geometries at the nano-scale, where simultaneous handling of local and non-local transport mechanisms over the particle surfaces must be realized. These phenomena are also of interest to several micro-fluidic applications including (but not limited to) lab-on-a-chip devices, micro-total analytic systems (μTAS) and point-of-care diagnostics (POC).

Abstract: The Knudsen paradox—the non-monotonous variation of mass-flow rate with the Knudsen number—is a unique and well-established signature of micro-channel rarefied flows. A particle which is not of insignificant size in relation to the duct geometry can significantly alter the flow behavior when introduced in such a system. In this work, we investigate the effects of a stationary particle on a micro-channel Poiseuille flow, from continuum to free-molecular conditions, using the direct simulation Monte-Carlo (DSMC) method. We establish a hydrodynamic basis for such an investigation by evaluating the flow around the particle and study the blockage effect on the Knudsen paradox. Our results show that with the presence of a particle this paradoxical behavior is altered. The effect is more significant as the particle becomes large and results from a shift towards relatively more ballistic molecular motion at shorter geometrical distances. The need to account for combinations of local and non-local transport effects in modeling reactive gas–solid flows in confined geometries at the nano-scale and in nanofabrication of model pore systems is discussed in relation to these results.

1. Introduction

A sub-micron sized particle when transported in a micro-channel can significantly alter the rarefied behavior of the carrier gas. These effects emerge partly because the dispersed particle serves as an extra momentum source or sink in the system and partly due to the blockage induced by the particle, which further affects the effective hydrodynamic length of the bounding duct. These phenomena are of particular significance from a theoretical view-point due to the complex molecular interactions that prevail at the aforementioned spatial scales, necessitating novel approaches to understand the same. Moreover, these challenging systems are also of interest to several micro-fluidic applications including (but not limited to) lab-on-a-chip devices, micro-total analytic systems (μTAS) and point-of-care diagnostics (POC) [1,2].

The Knudsen paradox [3–5] is a unique signature of micro-channel rarefied flows. Usually, such flows are characterized by the Knudsen number, $Kn = \lambda/a$, where λ is

the mean-free-path of the gas and a is a suitable system length scale (for instance, the channel height). Consequently, these flows can be classified into four regimes: continuum flows ($Kn < 0.001$), slip flows ($0.001 \leq Kn < 0.1$), transition flows ($0.1 \leq Kn < 10$) and free-molecular flows ($Kn \geq 10$) [6,7]. The Knudsen paradox is characterized by the variation in the mass-flow rate (Q) of a molecular gas in micro-channels across these aforementioned regimes, where the ratio between the length and hydraulic diameter is large. Note that the flow in these micro-channels is driven by the inlet-outlet pressure gradient. Correspondingly, in such systems, Q decreases with increasing Kn, reaches a minimum at $Kn \approx O(1)$ (in the transition regime) and further increases with an increase in Kn (towards the free-molecular regime). For this reason, the Knudsen paradox is also referred to in literature as the Knudsen minimum. The paradox was first studied experimentally and theoretically by Knudsen [3] in experiments of Poiseuille flow driven by the identical pressure drop in channels with varying widths. The observation of this minimum was attributed, by Pollard and Present [4], to the imbalance between two counteracting molecular effects–the obstruction of long diffusion paths due to molecular collisions, leading to a net decrease in Q on the one hand and the development of drift transport leading to an increase in Q on the other hand. Thus, it follows that Q in a long tube must initially decrease with increasing pressure (when $L > \lambda \gg a$, where L is the channel length) and pass through a minimum value due to the obstruction to molecular diffusion. As the pressure crosses this threshold ($\lambda < a$), drift transport increases (towards the Poiseuille form) leading to an increase in Q.

The Knudsen paradox has also been confirmed through numerical assessments, first by Cercignani and co-workers [5,8,9] and later by others (e.g., [10–12]). These authors solved the steady Boltzmann equation with a BGK (Bhatnagar–Gross–Krook) [13] collision term. For a detailed review of these approaches, the reader is referred to the book by Cercignani [14]. More recently, these numerical methods have been further extended and validated to handle a wide range of rarefied flows in a variety of geometries, as described in the reviews by Sharipov [15], Beskok [16], Karniadakis [17] and Colin [18]. In general, the reported methods are at the following levels of abstraction: (i) micro-scale resolved techniques that directly model molecular scale effects (such as inter-molecular and molecule-wall interactions); (ii) meso-scale resolved techniques (using the Boltzmann equation) that solve the molecular distribution function; and (iii) macro-scale (continuum) resolved techniques that incorporate velocity slip and temperature jump boundary conditions into the Navier–Stokes equations to model molecular phenomena. The continuum based methods are valid up to the transition regime [19], while the meso- and micro-scale methods can in principle be applied across the entire Kn range [6]. Thus, these two alternatives are preferred while evaluating the Knudsen paradox. Consequently, the lattice Boltzmann method (LBM) [20,21] and the direct simulation Monte-Carlo (DSMC) method [22,23] have gained prominence in rarefied micro-channel flow studies.

In general, research on single-phase rarefied Poiseuille flows are extensive (cf. [16–18]). However, related work on their multiphase counterparts (where a solid particle and a rarefied gas co-exist in the micro-channel) are relatively scarce. Currently, these reported multiphase studies are mostly limited to assessing stationary flow past a particle (e.g., [24–27]), indicative of a knowledge gap. In fact, investigations on the effect of an additional particulate phase on the Knudsen paradox noted in micro-channel Poiseuille flows (in the transition regime) have not been previously reported. An additional motive to study such rarefied particulate Poiseuille flows stems from the recent advancements in nanofabrication techniques. Novel nanofabricated reactor systems are increasingly used to study nanoscale reactive flows [28]. Such systems are often designed to mimic naturally occurring reactor geometries, such as individual pores inside a porous medium. Particles can either be dispersed (as in a gas–solid flow) or stationary (as in typical heterogeneous catalysis applications). A requirement for the existence of a Knudsen minimum is that the duct exhibits free paths for molecular motion that are much longer than the mean radius, a configuration which is typically not readily encountered in natural porous media [4]. However, due to restrictions

imposed by nanofabrication as well as increasing demand for advanced experimental equipment, artificial model pores may well fulfill these requirements and thus exhibit Knudsen minima effects.

Furthermore, the spatial variability in the heterogeneous topology of natural porous media has been shown to reduce the relevance of rarefaction effects on the total flow rate in the slip flow regime [29], which could imply that effects observed in systems with regular pore patterns may differ from the systems they are meant to represent. As model pore manufacturing methods are swiftly advancing, possibilities to experimentally investigate reactive rarefied gas–solid flows in model pores will soon become available. It is then of great interest to understand the differences in flow and transport characteristics of artificially designed systems to their intended natural counterparts. Such studies are particularly relevant for understanding pressure-driven transport of nanoparticles through micro-channels as encountered during reactive particulate matter flows in catalytic automobile exhaust after-treatment devices [27]. The physical scales studied here are also relevant for nanoparticle and dust transport in ambient to low-pressure environments inside natural porous media (such as ceramic substrates) or man-made electronics (such as printed circuit boards) [30–32]. This paper aims to address these open questions in rarefied Poiseuille flows with the simultaneous presence of a particulate phase. Consequently, we investigate the Knudsen paradox in a regular micro-channel Poiseuille flow with a stationary obstacle placed at its center and discuss the implications of our observations for reactive particulate flows.

The obstacle is intended to represent a particle which is not small in relation to the duct geometry. For simplicity, the particle is assumed to be square shaped, occupying the entire depth of the micro-channel and immobile. We use the DSMC method developed by Bird [22,23] for the respective assessments. This is an efficient particle-based (micro-scale) method that simulates interactions between molecular parcels, which represents groups of molecules having the same properties such as velocity and temperature. The relevant macroscopic quantities of the flow are extracted by statistically averaging over these microscopic quantities. Consequently, we employ the thoroughly validated open source DSMC solver *dsmcFoam+* (implemented within the *OpenFOAM* software framework [33]), developed by White and co-workers [34], for the simulations presented in this paper. We evaluate the variation of a normalized form of Q (referred to as Q_{norm}) across the entire Kn range in micro-channel Poiseuille flows with a particle. We investigate the effect of the particle size, in terms of a blockage ratio given as H/h, where H and h are the channel and particle heights, respectively, on the obtained Knudsen minimum. Additionally, the velocity along with the Mach number developed across the channel, are estimated to establish a hydrodynamic basis for the noted variation in Q_{norm}.

2. Problem Description

In this paper, we evaluate the pressure driven flow of rarefied nitrogen gas in a micro-channel. This is a Cartesian 2D planar setup with the flow along the x-direction. A stationary square-shaped particle is placed at the center of the micro-channel. We consider three different configurations, given by particle blockage ratios (or H/h where H and h are the micro-channel and particle heights, respectively) 8, 4 and 2, which represent progressively increasing degree of channel obstruction (see Figure 1). The channel length (L) is five times its height (H), which is is 0.4 μm, to ensure that a fully developed flow with minimal entrance effects can be realized. The pressure drop (ΔP) across the channel is varied so as to reasonably span over the entire Kn range. Such a fundamental setup is chosen since it perfectly mimics the flow configuration studied in [5,35,36] and is well suited to describe the Knudsen paradox in micro-channels.
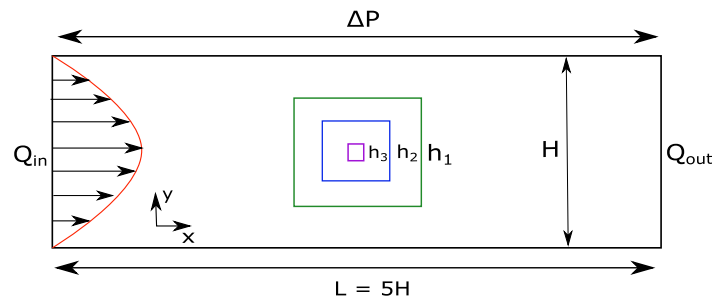
Figure 1. Schematic of the problem: 2D Planar Poiseuille flow in a micro-channel with a stationary obstacle in the middle. Note that the particle is square shaped with sides h1, h2 or h3 (decreasing in size), giving blockage ratios (H/h) 2, 4 and 8, respectively. The flow is along the x-direction.

3. DSMC Framework: $dsmcFoam+$

The direct simulation Monte-Carlo (DSMC), developed by Bird [23], is a stochastic particle-based technique for modeling real gases in which the molecular diameter is much smaller than the mean free path (λ). The primary objective of this method is to decouple molecular motion (modeled deterministically) and inter-molecular collision (modeled probabilistically) over small time intervals. The time interval over which the solution is sought is subdivided into smaller sub-intervals over which the particle motion and collisions are decoupled. Consequently, the trajectories are computed over a time interval which is lesser than the mean collision time. Further, DSMC relies on discrete parcels, which each contain a collection of molecules, to represent the total molecular number density (N) of the real gas. Thus, this method is computationally cheaper than a fully deterministic method like molecular dynamics (MD) and is ideally suited for studying rarefied gas dynamics [23].

We use the open-source solver $dsmcFoam+$ [34,36,37] for carrying out the assessments presented in this paper. This code-base is licensed under the GNU general public license with a publicly available software repository [38]. Further, it has been extensively validated against experimental and theoretical data across a wide variety of rarefied flows [34–36]. The algorithm employed in this solver can be summarized as follows. The flow domain is divided into cells (a Cartesian grid), which are in-turn populated with the DSMC parcels. Each of these parcels is assigned a position and a Maxwellian-distributed velocity based on the inlet conditions. Consequently, a Dirichlet type implicit boundary condition is used to assign the quantities associated with the molecules entering the computational domain (cf. [23,39]). The parcels are indexed into cells and arranged in an array to facilitate collisions. These parcels are then moved based on the type of interaction. Inter-molecular collisions are carried out probabilistically using the no-time counter (NTC) scheme proposed by Bird [23], while parcel-boundary interactions are simulated using a diffuse reflection model. The variable hard sphere (VHS) model [23] is used here to model the pair-wise collisions. The overall flow of molecules in the domain are driven by a downstream pressure outlet (Dirichlet type boundary condition for pressure, cf. [23,40]). These steps are repeated to increase the sample size until the statistical errors are small enough. Finally, the desired macroscopic flow properties are calculated by spatially and temporally averaging the sampled data. Note that, for the gas (di-atomic N_2) simulated in this study, the molecular collisions are considered elastic and they conserve both momentum and linear kinetic energy (of collision). For a more detailed account of the DSMC method and the $dsmcFoam+$ solver along with a detailed validation of the code, the reader is referred to [34,36,37].

4. Numerical Setup

The channel, considered in the DSMC simulations, has dimensions as shown in Figure 1 and is spatially discretized into $100 \times 60 \times 1$ computational cells along the x, y and z directions, respectively. Note that this is a pseudo-3D setup where the z direction is not solved for (i.e., a 2D planar simulation). This is done so as to mimic the setups of Cercignani et al. [5,8] and other similar studies [34–36]. A stationary obstacle (as shown

in Figure 1) is introduced in the center of the channel to obstruct the rarefied flow at varying degrees. This is given by particle blockage ratios (or H/h) 8, 4 and 2, which represent progressively increasing degree of channel obstruction. The surface and inlet temperatures are set to 300 K, while the inlet pressure is fixed based on the desired Kn (in our study, this varies from 5000 pa to 255,000 Pa). Further, the inlet to outlet pressure ratio is maintained at 3.0 for all the cases run (synonymous with the range prescribed in similar studies [34,35,37,41]). The time step size used in computing the DSMC parcel motion was determined smaller than the local mean collision time. The values of mass flow rate at the inlet and outlet are monitored until these are equivalent. The relevant macroscopic properties (e.g., temperature, density and velocity) are sampled after this steady state has been attained. The sampling is performed within each computational cell over a sufficiently large time step and over multiple realizations (to minimize statistical scattering) using relationships given by Hadjiconstantinou et al. [42]. These simulation conditions are summarized in Table 1.

Table 1. DSMC simulation conditions for a 2D planar micro-channel Poiseuille flow.

Property	Value
Gas	N_2
Mass (in Kg)	46.5×10^{-27}
Reference diameter (in m)	4.17×10^{-10}
Reference temperature (in K)	273
Viscosity index (ω)	0.74
Relaxation collision number	5.0
Particle blockage ratios (H/h)	8, 4 and 2
Micro-channel Aspect ratio (L/H)	5
Temperature (in K)	300
Inlet Pressure:P_{in} (in Pa)	varies from 5000 pa to 255000 Pa (based on the desired Kn)
Inlet/Outlet Pressure ratio	3
Time step (in s)	1.72×10^{-12}
Parcels per cell at the outlet	33

All gas properties were obtained from Bird's monograph [23].

A typical DSMC simulation is usually constrained by the following discretization criteria: (i) the computational cell size must be smaller than the local mean free path (if possible collision partners are restricted to a parcel's current cell); (ii) the number of parcels per cell must be large enough to preserve collision statistics; and (iii) the simulation time step must be chosen so that the parcels only cross a fraction of the average cell length during each time step. Conditions (ii) and (iii) are satisfied by employing a time-step much smaller than the mean collision time, while (i) is met by utilizing a spatial discretization that has already been validated exhaustively for the current setup (cf. [34–36]). All the simulations were carried out serially on a single node with 20 cores using an Intel® Xeon® (E5-2650) processor (up to 3.0 GHz). The simulations contained around 200,000 DSMC parcels in the case at a pressure of 255,000 Pa (each parcel has a weighting factor of 10). Note that the parcel count reduces as the pressure (and consequently the mass flow of the gas) in the micro-channel reduces. Hence, to minimize the statistical scatter in the collected data, two realizations of each DSMC simulation were run for a total of 100,000 sampling intervals. The results presented in this paper are ensemble averaged over these two realizations (the scatter was noticeably reduced). Furthermore, the velocity extracted from the simulation (shown in Figure 2) is displayed both using the scattered raw data as well as a polynomial fitted using a weighted least squares estimate [43], so as to facilitate a simplified visualization of the data. Each DSMC simulation needed a physical time of 100 h.
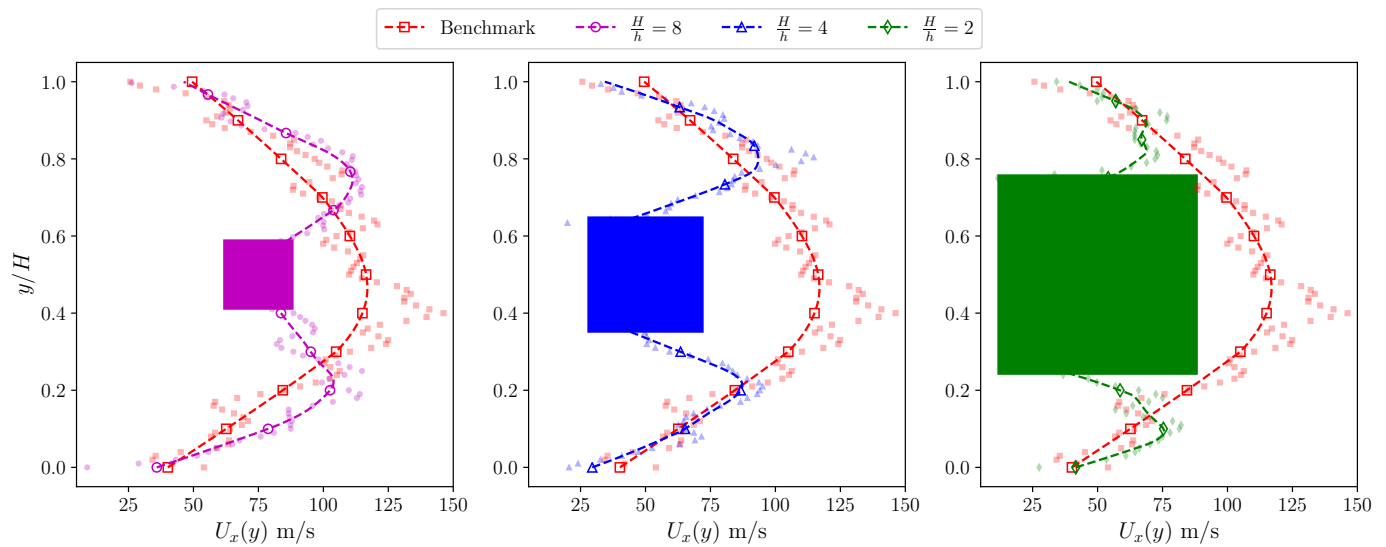
Figure 2. Comparison of the variations in co-axial velocity in the transition regime (*Kn* = 0.1) along channel height *H* at the center of the channel *x*/*L* = 0.5 across the chosen blockage ratios *H*/*h* of 8, 4 and 2, respectively, with the benchmark case without a particle (represented by the dashed line with squares). In this figure, the square particle is used as an illustrative tool to mask the discontinuities in the region occupied by the particle. The open symbols represent the DSMC data, while the dashed lines represent the weighted least squares fit.

5. Results and Discussion

We assess the Knudsen paradox in the numerical setup described above by varying the inlet pressure (P_{in}) and maintaining the inlet to outlet pressure ratio as 3. To compare our DSMC results to the results from Cercignani et al. [5,8], the mass flow rate *Q* (obtained from the simulations) is represented in a non-dimensional form. This dimensionless flow rate Q_{norm} used is [34,41]:

$$Q_{norm} = \frac{\dot{m}L\sqrt{2RT}}{H^2 w (P_{in} - P_o)} \tag{1}$$

where *L*, *H* and *w* are the length, height and width of the micro-channel, respectively. Further, *R* and *T* are the specific gas constant and iso-thermal temperature of the gas. The variable $\dot{m}$ is the mass flux extracted by the *dsmcFoam+* solver (using the mass flux measurement tool described in [34]) and P_{in} and P_o are the inlet and outlet pressures. Note that Q_{norm} is independent of the local pressure gradient (depends only on its mean value), but depends mainly on the channel height represented in terms of a rarefaction parameter δ_m (i.e., on an inverse Knudsen number—λ/H) [41] given by:

$$\delta_m = \frac{\sqrt{\pi}}{2Kn} \tag{2}$$

Equations (1) and (2) can be used to describe the rarefied flow with the particle as well under the same constraints, i.e., the local pressure gradient (defined as $\frac{H}{P}\frac{dP}{dx}$) is small (or $\ll$ 1). Correspondingly, we show the comparisons between *dsmcFoam+* and the data of Cercignani et al. [5,8], along with the effect of particle blockage on the Knudsen paradox. Prior to this discussion, we first establish a hydrodynamic basis for the effect of the stationary particle in the channel. This is done by comparing the corresponding velocity profiles across the micro-channel setups with and without the particle in the transition regime (at *Kn* = 0.1). We also briefly evaluate the compressibility effects of the particle on the flow system by examining the Mach number developed in in this flow regime.

5.1. Hydrodynamics of a Stationary Particle in the Transition Regime

The presence of a stationary and inert particle in a 2D planar micro-channel Poiseuille flow of a rarefied gas in the transition regime alters the inherent response of the system. This is because of the additional momentum sink in the flow due to the particle. We investigate the hydrodynamic consequences of such a flow obstruction by comparing the velocity in the micro-channel with a benchmark case without the particle. Such an assessment has a two-fold objective: (i) deviations from the ideal micro-channel Poiseuille flow due to the presence of the particle can be identified; and (ii) the hydrodynamic basis for the observed Knudsen paradox can be deduced. We first discuss the impacts on the channel velocity profile (along the height) and follow this with a brief discussion on the compressibility of such particulate flows. Note that all these hydrodynamic assessments are done under the conditions defined in Table 1 and at an outlet pressure P_o of 1 bar ($Kn = 0.1$). This Kn is chosen as it represents the unique hydrodynamics in the transition regime, where the Knudsen minimum has been observed in micro-channel Poiseuille flows [5,41].

The 2D planar micro-channel Poiseuille flow benchmark case without the particle is characterized by a parabolic velocity profile. Consequently, when the flow encounters a stationary particle at the center of the channel, its response is markedly altered. Figure 2 shows the variation of the co-axial velocity along the y-direction ($U_x(y)$). As expected, the presence of the particle decelerates the overall flow, with the maximum velocity reduced due to the blockage. It follows that, at the center of the channel, the particle partitions the flow into two narrower channels each developing its own parabolic velocity profile for $U_x(y)$, with a maximum velocity lower than the benchmark case. Note that velocities at the wall boundaries are always nonzero due to a net slip-effect in the transition regime. The non-uniformities noted in the reported velocity profiles are attributed to the statistical scatter from the DSMC data. This scatter is more visible at the lowest blockage ratios as the largest particle drastically alters the local length scale of the system, thereby decreasing the probability of molecular collisions in this region, which in turn increases the need for sampling to converge the statistics. Nevertheless, the results obtained for the lowest blockage ratio are deemed reasonable enough as they follow the expected trend despite the scatter. These observations are further confirmed by the streamlines of the velocity along a $x - y$ plane, shown in terms of the Mach number ($Ma = u/c$, where u is the local fluid velocity and c is the speed of sound) in Figure 3. The flow accelerates as it passes the particle, partly due to the pressure decrease but mostly due to continuity. Further, a symmetric low-velocity region is developed before and after the particle. The channeling effect created by the presence of the particle has a consequent impact on the Knudsen paradox, as will be explained later.

Furthermore, the mach number (Ma) is also used to assess compressibility effects in a flow system [44], where such effects are generally deemed negligible for $Ma < 0.3$. This criterion may however be violated in micro-channel Poiseuille flows. Figure 3 shows Ma in the micro-channel for all cases with and without the particle at the conditions reported in Table 1. The benchmark case shows that such Poiseuille flows are sub-sonic in nature with $Ma < 0.8$. The highest Ma is observed at the flow outlet as expected. The additional momentum sink, due to the particle, leads to a lower flow velocity of the rarefied gas at the outlet and as the particle size increases, there is a corresponding decrease in the developed Ma. Thus, compressibility effects can be disregarded while assessing micro-channel Poiseuille flows with a stationary particle with a non-negligible size in relation to the duct geometry (at the same driving pressure difference). This is an important observation for numerically representing such systems, as a constant density can be assumed while setting up the study.
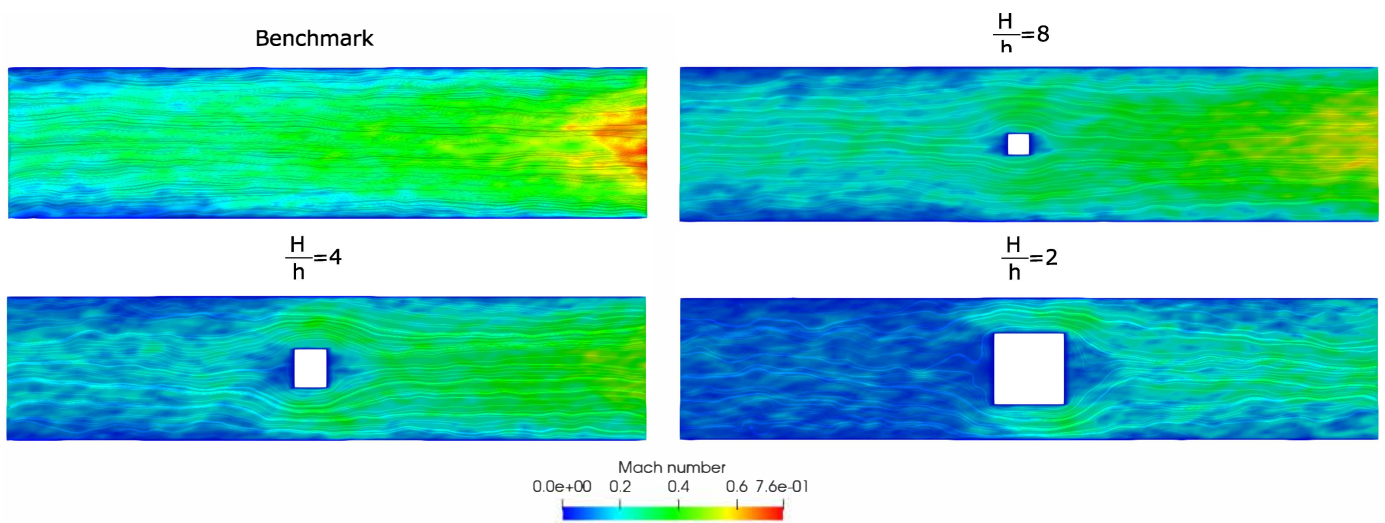
Figure 3. Contours of Mach number (*Ma*), overlaid with velocity streamlines (colored by *Ma*), along an $x - y$ plane for the benchmark case (see Table 1) and the DSMC simulations at blockage ratios H/h of 8, 4 and 2, respectively.

5.2. Effect of the Particle on the Knudsen Paradox

We assess the Knudsen paradox in the 2D setup (described in Figure 1) by varying the inlet pressure (P_{in}) and maintaining the inlet to outlet pressure ratio as 3. As detailed above, the normalized mass flow rate in the channel Q_{norm} (see Equation (1)) is extracted from the DSMC simulations across the entire Kn range, i.e., at different δ_m (which is in turn related to Kn as shown in Equation (2)). Figure 4 shows the Knudsen minima estimated from the DSMC simulations along with inherent uncertainties in the sampled data (through error bars). In this figure, the solid lines represent cases without a particle, while the dashed lines represent the cases with one. The comparisons between the benchmark case (without a particle) and the results given by Cercignani et al. [5,8] are reasonable, given the statistical spread of the sampled data. The agreement is good at high δ_m (or low Kn) values with a deviation noted at the lower ones. The result in this region is more sensitive to the scatter in the DSMC data (indicated by the wider error bars in this region) and is also known to be affected by the lateral boundary condition in pseudo-3D systems [45]. However, these obtained results clearly depict the Knudsen paradox (within the limits of certainty of the simulation setup) and are synonymous with those reported by White et al. [34] using the same solver. Moreover, the minima is noted at $\delta_m = 0.97$ (which is at around $Kn \approx 1$, i.e., in the transition regime), as reported by others (cf. [5,8,41]). The predicted Knudsen minima for all the cases simulated are summarized in Table 2.

When a particle is introduced in the channel, it serves as an additional momentum sink in the system and sections of high fluid velocity are created in the regions between the particle and wall (see Figure 3). The Knudsen minimum may have shifted towards higher Knudsen numbers (see Table 2), although our data does not provide enough statistical confidence to confirm this. Nevertheless, the noted trends could be due to a shift towards relatively more ballistic molecules (that do not collide with each other) at shorter geometrical distances—a trend similar to that observed when going from a channel flow to a duct flow [45] or with flows in a bent channel [46]. In other words, the presence of the particle reduces the governing local length scales of the system, with a decreased probability of molecular interactions along the diffusion paths of the gas molecules. Moreover, the momentum sink effect causes the total mass flow rate in the channel to be reduced. Such a reduction in Q_{norm} is noticeable in Figure 4, with lower mass flows noted as the particle size increases, thereby effectively blocking the channel to a higher degree. It can also be noted that the relative changes in Q_{norm} with increasing particle size in the transition regime diminishes, with the curve tending to flatten out. This occurs as beyond the continuum regime the frictional losses become relatively less important due to velocity slip.

Moreover, as the particle becomes larger, there is an increased chance that the Knudsen paradox totally disappears, which means that Q_{norm} monotonically decreases without any increase at higher Kn (or lower δ_m) similar to observations made in bent channels by Liu et al. [46]. Synonymous with the inferences drawn from the bent channel studies, we also attribute the observed behavior to the apparent increase in the local hydrodynamic resistances due to the particle. Thus, the global mass flow rate is now determined by the momentum loss imposed by the stationary particle and in this region the free paths for molecular motion are not longer than the mean channel height anymore. Note that on the basis of our data the blockage ratio (H/h) of 2 could represent a limiting case for the transition from a single to a multiple channel system (due to the partitioning effect of the flow from the particle). Such a channel system could possibly be characterized by a Knudsen number which is four times that of the upstream duct. Indeed, the transition is found (see Table 2) to occur at around $Kn \approx 5$ which supports this hypothesis, given the scatter in the data.
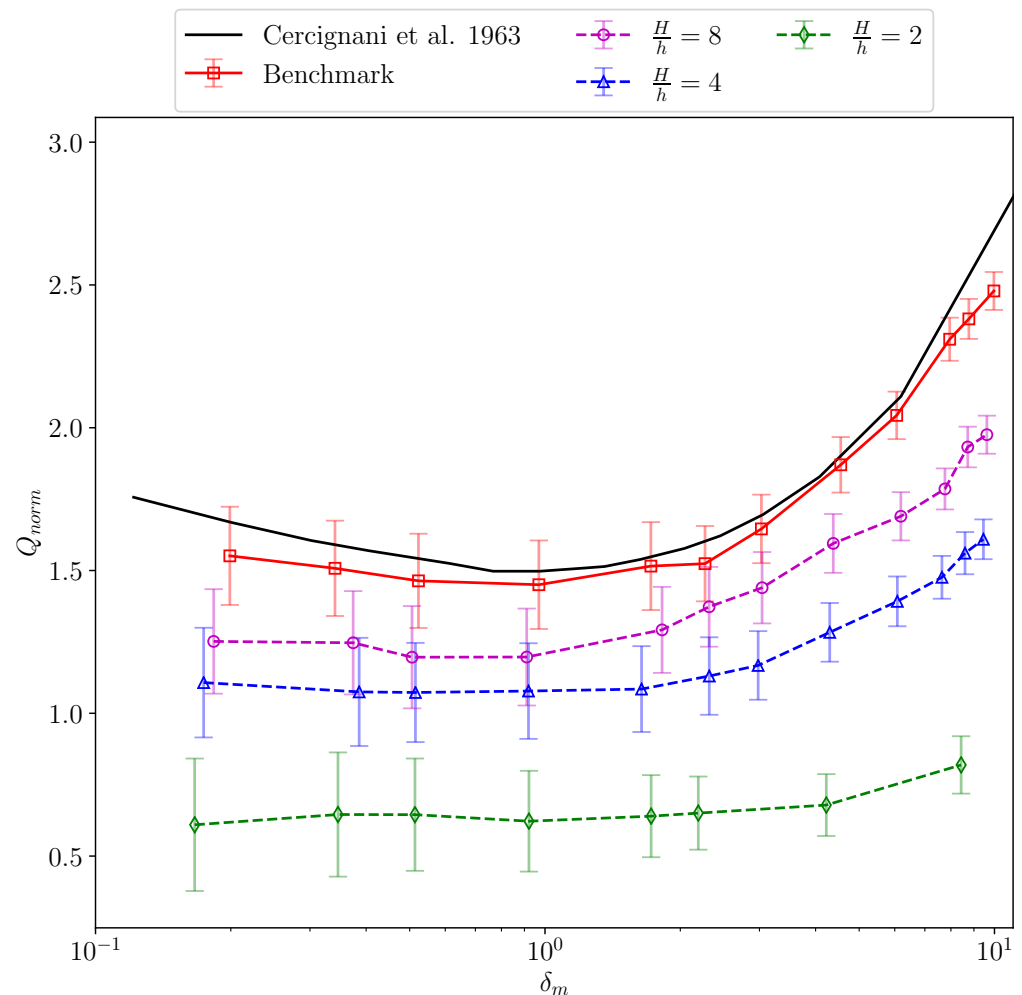

Figure 4. Knudsen paradox in 2D planar micro-channel Poiseuille flows with a stationary particle in the middle. The solid line (——) represents the results obtained by Cercignani et al. [5,8], while the red line (——) with open squares represents the benchmark results (without a particle). The dashed lines represent the results obtained from the DSMC simulations of a micro-channel at blockage ratios H/h of 8, 4 and 2, respectively. The error bars indicate the statistical spread (± 1 standard deviation) in the sampled data. Note that the error bars increase as H/h decreases (or the particle size increases) since the local Knudsen number in the restrictions created by the particle is higher.

Table 2. Knudsen minimum in 2D planar micro-channel Poiseuille flows with a stationary particle in the middle. Note that the reported minima is subject to the variations in the sampled data shown in Figure 4.

Case	δ_m	Kn
Cercignani et al. [5,8,9]	0.77	1.16
Benchmark (without particle)	0.97	0.92
$H/h = 8$	0.38	2.32
$H/h = 4$	0.36	2.46
$H/h = 2$	0.17	5.34

5.3. Implications for Reactive Particulate Flows

The assessments presented in this paper are particularly relevant when studying local mass diffusivities in the transition regime. In such studies, the local mass diffusivity becomes influenced by the particle-to-wall distance and the determination of a local diffusivity (for example, in the region between the particle and the wall) requires a local Kn [47]. Both the continuum approximation and the assumption of thermodynamic quasi-equilibrium break down at finite Kn [15,48], implying that completely different mechanisms may govern mass transfer on different sides of an asymmetrically positioned particle.

It has also been shown that the mass transfer coefficient in pressure-driven channel flows at varying degrees of rarefaction is essentially constant with Kn, whereas the heat transfer coefficient is strongly dependent on Kn, leading to a breakdown of the well-known heat and mass transfer analogies [49]. This difference in behavior originates from the non-local transfer phenomena: whereas a molecule coming from a distant region with a significantly different temperature is able to transfer a significantly different energy load (to the molecules in the near-particle region), the mass transfer capability of any given molecule is always the same, independent of the region from which the molecule originates [49]. Moreover, for nanofabricated systems with parallel channels the existence of Knudsen minima implies that the mass-flow rate through a given channel may vary non-monotonously with the degree of rarefaction in the transition regime. As the local rarefaction will depend on the local blockage and particle-wall distances for a gas–solid flow and as these may exhibit highly dynamic characteristics, oscillations in flow rate (and thus in retention time) may be expected to arise spontaneously under certain conditions. For reactive systems, where particle sizes change continuously due to chemical reactions, and which may be controlled by either mass or heat transfer or chemical kinetics, controlling the non-local transport characteristics may thus require accounting for highly complex Knudsen minima effects.

The local mass diffusivity in a reactive nano-scale system will thus depend on the local flow configuration. The present work demonstrates that, for an immobile particle, the Knudsen paradox may offer a possibility to indirectly assess or characterize these phenomena from the response of the global mass-flow rate to variations in the absolute pressure. Finally, for a suspended particle that is moving with the average gas flow velocity, the momentum sink effect may become insignificant, but the effects of the local length-scale reduction will remain in full. The latter effects are also the most relevant for nano-scale reactive flows.

6. Conclusions

In this paper, we present a DSMC investigation of the effect of a stationary particle on the Knudsen paradox observed in micro-channel Poiseuille flows. Such an investigation has previously not been reported in the literature. The objective with this study was to assess the effects from representing natural porous media through nanofabricated model pores in rarefied gas–solid systems and heterogeneous catalysis applications. The open source solver *dsmcFoam+* was used to carry out the relevant studies. We show that the presence of a particle markedly alters the response of the rarefied flow system as it serves as

an additional momentum sink in the flow. Further, as it becomes larger and subsequently blocks a larger portion of the duct (represented as the blockage ratios H/h), the mass-flow rate at the same nominal pressure difference decreases. Despite the noticeable scatter in the reported data, the general trends (in Q_{norm}) observed agree with conventional rarefied flow dynamics in micro-channels and parallelisms can be drawn from our study and that of Liu et al. [46] on micro-channels with bends. In both assessments, an increase in the local hydrodynamic resistances in the flow leads to noticeable deviations from the behavior derived for straight micro-channel Poiseuille flows by Cercignani et al. [5]. Consequently, with the presence of a particle, the Knudsen minimum is shifted towards higher Knudsen numbers with the curve flattening out towards the free-molecular flow regime. This effect is more pronounced as the particle becomes large and it results from a shift towards relatively more ballistic molecular motion at shorter geometrical distances. These observations have significant implications for the design of model pore systems for reactive rarefied gas–solid flows, as well as investigations of heterogeneous catalysis using stationary catalyst particles. Most notably, the local mass diffusivity, which determines the overall reaction rate at mass-transfer limited conditions, will depend on the local flow configuration, which may thus be indirectly assessed from the response of the global mass-flow rate as a function of absolute pressure. Moreover, attention should be paid to the possibility for flow oscillations to manifest in nano-scale reactor systems with rarefied reactive gas–solid flow.

In conclusion, the present work addresses a perceived knowledge gap in rarefied flows along with a relevant challenge while modeling reactive gas–solid flows in confined geometries at the nano-scale, where simultaneous handling of local and non-local transport mechanisms over the particle surfaces must be realized. The observed trends can be extended towards asymmetric particles as well, since the presence of any particle in the flow increases the overall hydrodynamic resistances in it. Thus, we underline the need to account for these complex transition regime effects while assessing such rarefied gas–particle systems, particularly in the relevant micro-fluidic applications.

Abbreviations

The following abbreviations are used in this manuscript:

BGK	Bhatnagar–Gross–Krook
DSMC	Direct simulation Monte-Carlo
GNU	General Public License
MD	Molecular dynamics
μTAS	Micro-total analytic systems
NTC	No-time counter
OpenFOAM	Open-source Field Operation And Manipulation
POC	Point-of-care diagnostics
VHS	Variable hard sphere

References

1. Sajeesh, P.; Sen, A.K. Particle separation and sorting in microfluidic devices: A review. *Microfluid. Nanofluid.* **2014**, *17*, 1–52. [CrossRef]
2. Bayareh, M. An updated review on particle separation in passive microfluidic devices. *Chem. Eng. Process. Process Intensif.* **2020**, *153*, 107984. [CrossRef]
3. Knudsen, M. Die Gesetze der Molekularströmung und der inneren Reibungsströmung der Gase durch Röhren. *Ann. Phys.* **1909**, *333*, 75–130. [CrossRef]
4. Pollard, W.G.; Present, R.D. On Gaseous Self-Diffusion in Long Capillary Tubes. *Phys. Rev.* **1948**, *73*, 762–774. [CrossRef]
5. Cercignani, C.; Daneri, A. Flow of a Rarefied Gas between Two Parallel Plates. *J. Appl. Phys.* **1963**, *34*, 3509–3513. [CrossRef]
6. Barber, R.W.; Emerson, D.R. Challenges in Modeling Gas-Phase Flow in Microchannels: From Slip to Transition. *Heat Transf. Eng.* **2006**, *27*, 3–12. [CrossRef]
7. Agrawal, A. A Comprehensive Review on Gas Flow in Microchannels. *Int. J. Micro-Nano Scale Transp.* **2007**, *2*, 3411–3421. [CrossRef]
8. Cercignani, C. *Plane Poiseuille Flow and Knudsen Minimum Effect*; Academic Press: New York, NY, USA, 1963; Volume 2, pp. 92–101.
9. Cercignani, C.; Sernagiotto, F. Cylindrical Poiseuille Flow of a Rarefied Gas. *Phys. Fluids* **1966**, *9*, 40–44. [CrossRef]
10. Huang, A.B.; Stoy, R.L. Rarefied Gas Channel Flows for Three Molecular Models. *Phys. Fluids* **1966**, *9*, 2327–2336. [CrossRef]
11. Loyalka, S.K.; Ferziger, J.H. Model Dependence of the Slip Coefficient. *Phys. Fluids* **1967**, *10*, 1833–1839. [CrossRef]
12. Ferziger, J.H. Flow of a Rarefied Gas through a Cylindrical Tube. *Phys. Fluids* **1967**, *10*, 1448–1453. [CrossRef]
13. Bhatnagar, P.L.; Gross, E.P.; Krook, M. A Model for Collision Processes in Gases. I. Small Amplitude Processes in Charged and Neutral One-Component Systems. *Phys. Rev.* **1954**, *94*, 511–525. [CrossRef]
14. Cercignani, C. *The Boltzmann Equation and Its Applications*; Applied Mathematical Sciences Book Series (AMS); Springer: New York, NY, USA, 1988; Volume 67; doi:10.1007/978-1-4612-1039-9. [CrossRef]
15. Sharipov, F.; Seleznev, V. Data on Internal Rarefied Gas Flows. *J. Phys. Chem. Ref. Data* **1998**, *27*, 657–706. [CrossRef]
16. Ali Beskok, G.E.K. Report: A model for flows in channels, pipes, and ducts at micro and nano scales. *Microscale Thermophys. Eng.* **1999**, *3*, 43–77. [CrossRef]
17. Karniadakis, G.E.; Beskok, A.; Gad-el Hak, M. Micro Flows: Fundamentals and Simulation. *Appl. Mech. Rev.* **2002**, *55*, B76–B76. [CrossRef]
18. Colin, S. Rarefaction and compressibility effects on steady and transient gas flows in microchannels. *Microfluid. Nanofluid.* **2005**, *1*, 268–279. [CrossRef]
19. Arkilic, E.B.; Schmidt, M.A.; Breuer, K.S. Gaseous slip flow in long microchannels. *J. Microelectromech. Syst.* **1997**, *6*, 167–178. [CrossRef]
20. Chen, S.; Doolen, G.D. Lattice boltzmann method for fluid flows. *Annu. Rev. Fluid Mech.* **1998**, *30*, 329–364. doi:10.1146/annurev.fluid.30.1.329. [CrossRef]
21. Agrawal, A.; Djenidi, L.; Antonia, R.A. Simulation of gas flow in microchannels with a sudden expansion or contraction. *J. Fluid Mech.* **2005**, *530*, 135–144. [CrossRef]
22. Bird, G.A. Monte Carlo Simulation of Gas Flows. *Annu. Rev. Fluid Mech.* **1978**, *10*, 11–31. [CrossRef]
23. Bird, G.A. *The DSMC Method*; CreateSpace Independent Publishing Platform: Scotts Valley, CA, USA, 2013.
24. Beresnev, S.A.; Chernyak, V.G.; Suetin, P.E. Motion of a spherical particle in a rarefied gas. Part 1. A liquid particle in its saturated vapour. *J. Fluid Mech.* **1987**, *176*, 295–310. [CrossRef]
25. Ström, H.; Sasic, S.; Andersson, B. A novel multiphase DNS approach for handling solid particles in a rarefied gas. *Int. J. Multiph. Flow* **2011**, *37*, 906–918. [CrossRef]
26. Corson, J.; Mulholland, G.; Zachariah, M. Hydrodynamic interactions between aerosol particles in the transition regime. *J. Fluid Mech.* **2018**, *855*, 535–553. [CrossRef]
27. Kannan, A.S.; Naserentin, V.; Mark, A.; Maggiolo, D.; Sardina, G.; Sasic, S.; Ström, H. A continuum-based multiphase DNS method for studying the Brownian dynamics of soot particles in a rarefied gas. *Chem. Eng. Sci.* **2019**, *210*, 115229. [CrossRef]
28. Albinsson, D.; Bartling, S.; Nilsson, S.; Ström, H.; Fritzsche, J.; Langhammer, C. Operando detection of single nanoparticle activity dynamics inside a model pore catalyst material. *Sci. Adv.* **2020**, *6*, eaba7678. [CrossRef]
29. Pérez-Ràfols, F.; Forsberg, F.; Hellström, G.; Almqvist, A. A Stochastic Two-Scale Model for Rarefied Gas Flow in Highly Heterogeneous Porous Media. *Transp. Porous Media* **2020**. [CrossRef]

30. Tencer, M. Deposition of aerosol ("hygroscopic dust") on electronics—Mechanism and risk. *Microelectron. Reliab.* **2008**, *48*, 584–593. [CrossRef]

31. Sobrado, J.M.; Martín-Soler, J.; Martín-Gago, J.A. Mimicking Martian dust: An in-vacuum dust deposition system for testing the ultraviolet sensors on the Curiosity rover. *Rev. Sci. Instrum.* **2015**, *86*, 105113. [CrossRef]

32. Matte-Deschênes, G.; Vidal, D.; Bertrand, F.; Hayes, R.E. Numerical investigation of the impact of thermophoresis on the capture efficiency of diesel particulate filters. *Can. J. Chem. Eng.* **2016**, *94*, 291–303. [CrossRef]

33. Weller, H.G.; Tabor, G.; Jasak, H.; Fureby, C. A tensorial approach to computational continuum mechanics using object-oriented techniques. *Comput. Phys.* **1998**, *12*, 620–631. [CrossRef]

34. White, C.; Borg, M.; Scanlon, T.; Longshaw, S.; John, B.; Emerson, D.; Reese, J. dsmcFoam+: An OpenFOAM based direct simulation Monte Carlo solver. *Comput. Phys. Commun.* **2018**, *224*, 22–43. [CrossRef]

35. Roohi, E.; Darbandi, M.; Mirjalili, V. Direct Simulation Monte Carlo Solution of Subsonic Flow Through Micro/Nanoscale Channels. *J. Heat Transf.* **2009**, *131*. [CrossRef]

36. White, C.; Borg, M.K.; Scanlon, T.J.; Reese, J.M. A DSMC investigation of gas flows in micro-channels with bends. *Comput. Fluids* **2013**, *71*, 261–271. [CrossRef]

37. Scanlon, T.J.; Roohi, E.; White, C.; Darbandi, M.; Reese, J.M. An open source, parallel DSMC code for rarefied gas flows in arbitrary geometries. *Comput. Fluids* **2010**, *39*, 2078–2089. [CrossRef]

38. White, C.; Borg, M.; Longshaw, S. MicroNanoFlows: OpenFOAM-2.4.0-MNF. 2018. Available online: https://github.com/MicroNanoFlows/OpenFOAM-2.4.0-MNF (accessed on 3 April 2020).

39. Wang, M.; Li, Z. Simulations for gas flows in microgeometries using the direct simulation Monte Carlo method. *Int. J. Heat Fluid Flow* **2004**, *25*, 975–985. [CrossRef]

40. Liou, W.W.; Fang, Y.C. Implicit Boundary Conditions for Direct Simulation Monte Carlo Method in MEMS Flow Predictions. *Comput. Model. Eng. Sci.* **2000**, *1*, 119–128. [CrossRef]

41. Ewart, T.; Perrier, P.; Graur, I.A.; Meolans, J.G. Mass flow rate measurements in a microchannel, from hydrodynamic to near free molecular regimes. *J. Fluid Mech.* **2007**, *584*, 337–356. [CrossRef]

42. Hadjiconstantinou, N.G.; Garcia, A.L.; Bazant, M.Z.; He, G. Statistical error in particle simulations of hydrodynamic phenomena. *J. Comput. Phys.* **2003**, *187*, 274–297. [CrossRef]

43. Cleveland, W.S. Robust Locally Weighted Regression and Smoothing Scatterplots. *J. Am. Stat. Assoc.* **1979**, *74*, 829–836. [CrossRef]

44. White, F. *Fluid Mechanics*; McGraw-Hill Series in Mechanical Engineering; McGraw Hill: New York, NY, USA, 2011.

45. Tatsios, G.; Stefanov, S.K.; Valougeorgis, D. Predicting the Knudsen paradox in long capillaries by decomposing the flow into ballistic and collision parts. *Phys. Rev. E* **2015**, *91*, 061001. [CrossRef]

46. Liu, W.; Tang, G.; Su, W.; Wu, L.; Zhang, Y. Rarefaction throttling effect: Influence of the bend in micro-channel gaseous flow. *Phys. Fluids* **2018**, *30*, 082002. [CrossRef]

47. Yang, G.; Weigand, B. Investigation of the Klinkenberg effect in a micro/nanoporous medium by direct simulation Monte Carlo method. *Phys. Rev. Fluids* **2018**, *3*, 044201. [CrossRef]

48. Gad-El-Hak, M. Gas and Liquid Transport at the Microscale. *Heat Transf. Eng.* **2006**, *27*, 13–29. [CrossRef]

49. Bond, D.; Goldsworthy, M.; Wheatley, V. Numerical investigation of the heat and mass transfer analogy in rarefied gas flows. *Int. J. Heat Mass Transf.* **2015**, *85*, 971–986. [CrossRef]